Computational Fluid Dynamics Simulation with Lattice Boltzmann Technique.*

Nures Saba Tiana[1] [nures.saba.tiana@g.bracu.ac.bd]
, Azrin Hossain[1] [azrin.hossain@g.bracu.ac.bd]
, Afrin Binta Amzad[1] [afrin.binta.amzad@g.bracu.ac.bd]
, Ashiful Hasan Shadman[1] [ashiful.hasan.shadman@g.bracu.ac.bd]
, Annajiat Alim Rasel[1] [annajiat@gmail.com]
, Mehnaz Ara Fazal[1] [mehnaz.ara.fazal@g.bracu.ac.bd]
, and Adib Muhammad Amit[1] [adib.muhammad.amit@g.bracu.ac.bd]

BRAC University

Abstract. This paper presents a comprehensive exploration of the significance of Computational Fluid Dynamics (CFD) in analyzing hydraulic environments, environmental problems, and aerodynamics. The study highlights the role of CFD in investigating hemodynamics, predicting stability derivatives, and optimizing engineering systems such as centrifugal compressors, heat exchangers, and pharmaceutical processors. Furthermore, the paper discusses the real-world applications of CFD in diverse fields, including wind engineering, building performance simulation, and battery pack thermal modeling. The Lattice Boltzmann Technique is employed to simulate fluid dynamics, providing a dynamic depiction of complex fluid phenomena. Through the real-time visualization of vorticity, the technique contributes to the comprehensive exploration of fluid dynamics. The paper emphasizes the paramount importance of understanding and predictive modeling of K´arm´an vortex streets in various engineering and scientific domains, facilitating the optimization of structural designs and the enhancement of fluid flow efficiency. Overall, this paper underscores the crucial role of CFD and the Lattice Boltzmann Technique in addressing a wide range of practical problems and advancing scientific understanding of fluid dynamics.

Keywords: Computational Fluid Dynamics · Lattice Boltzmann Technique · Vorticity visualization · Karman vortex streets

1 Introduction

The significance of Computational Fluid Dynamics (CFD) lies in its ability to analyze hydraulic environments, environmental problems, and aerodynamics, as well as to investigate flow over spillways, monitor and analyze pollutants, and study the dynamics of air-water interaction (Chinnarasri et al., 2014; Yu et al., 2017; Orfánus & Rumann, 2019; Sforza et al., 2011; Ochi et al., 2010). CFD

* Supported by BRAC University.

is also crucial in investigating the role of hemodynamics in cerebral aneurysms and predicting stability derivatives for airships and airfoils (Wang, 2012; Fang et al., 2023; Aydin et al., 2017). Furthermore, CFD plays a significant role in the design and optimization of various engineering systems, such as centrifugal compressors, heat exchangers, and pharmaceutical processors (Macgregor et al., 1999; Amirante et al., 2007; Xu et al., 2014). It is also used in evaluating the flow forces on valves, optimizing downhole float valves, and investigating the impact of cold spots on subsea insulation performance (Taxy & Lebreton, 2004; Kim et al., 2019; Liu et al., 2015).

Moreover, CFD has been applied in diverse fields, including wind engineering, building performance simulation, and battery pack thermal modeling (Lin et al., 2011; Hu & Zhang, 2018; Zhu et al., 2018). It has also been used to study the combustion of energetic materials, evaluate the flow rate and torques of control valves, and predict the aerodynamic loads on space launch vehicle systems (Applebaum et al., 2012; Pratama & Bramantya, 2018; Lu et al., 2011). Additionally, CFD has been employed in the analysis of the dynamics of safety relief valves, the thermal analysis of subsea equipment, and the optimization of air supply in enclosed environments (Chen, 2009; Hu & Zhang, 2018).

The use of CFD is not without challenges, as it can be time-consuming and computationally expensive (Macgregor et al., 1999). However, with advancements in computer performance, unsteady CFD analysis has become more feasible, and steady-state CFD analysis continues to be successful in the field of aerodynamics (Ochi et al., 2010). Overall, the importance of CFD lies in its wide-ranging applications across various disciplines, its ability to optimize engineering systems, and its potential to address complex fluid-thermal coupling effects.

1.1 Fluid Dynamics on Lattice

The Lattice Boltzmann Method (LBM) is a computational method that has gained prominence for simulating complex states of flowing matter across various scales, from fully developed turbulence to multiphase micro-flows, and even quantum-relativistic subnuclear fluids (Chinnarasri et al., 2014; Yu et al., 2017). It is based on the microscopic and kinetic theory of gases, allowing for the simulation of fluid dynamics and the constitutive equations of viscoelastic fluids (Chen, 2009; Hu & Zhang, 2018). Additionally, the LBM has been successfully applied to simulate fluid-solid interactions, enabling the study of wetting effects and contact line dynamics (Zhang, 2018).

Furthermore, the LBM has been utilized in the simulation of plume dynamics, demonstrating its applicability in geophysical studies (Luo et al., 2017). Its versatility is further highlighted by its use in simulating wind-solar energy harvesting, where it was coupled with a finite element structural solver to minimize simulation run time (Luo et al., 2017). Moreover, the LBM has been employed in the study of flexibility and inertial effects on the deformation and cruising reversal of self-propelled flexible swimming bodies, showcasing its relevance in the field of materials science and mechanics (Belyaev, 2017).

The accuracy of LBM simulations is enhanced by considering the correct implementation of fluctuations in mesoscopic methods, which is crucial for understanding large fluctuations in nonideal coarse-grained systems (Montessori et al., 2020). Additionally, the comparison of lattice gas with molecular dynamics collision operators has provided insights into the expressions for temperature and pressure in LBM simulations, emphasizing the importance of accurate identification in the modeling process (Ma et al., 2020; Luo et al., 2017).

In conclusion, the Lattice Boltzmann Method plays a crucial role in fluid dynamics simulation due to its efficiency, accuracy, and versatility in modeling complex fluid flow phenomena across various disciplines, from geophysics to materials science.

1.2 Objectives

The primary objective of this study is to delve into the intricate dynamics of fluid movement through the lens of the Lattice Boltzmann method in computational fluid dynamics (CFD). By embarking on a comprehensive simulation journey, the aim is to gain a nuanced understanding of fluid behavior at both microscopic and macroscopic scales. The utilization of the Lattice Boltzmann method provides a unique vantage point, offering a detailed and efficient framework to simulate fluid flow. Through the course of the simulation, the intricate interplay between streaming and collision processes will be meticulously observed, shedding light on the emergence of macroscopic fluid phenomena.

The simulation unfolds in a stepwise manner, from the initialization of lattice parameters and conditions to the incorporation of boundary conditions and the refinement of the model. The introduction of a solid cylinder further adds complexity, allowing for the exploration of boundary interactions. Visualization techniques, such as the calculation of curl to represent vorticity, enhance the interpretability of the simulated fluid movement. The overarching goal is to glean insights into the fluid's intricate dynamics, providing a valuable foundation for further advancements in computational fluid dynamics and contributing to the broader understanding of fluid behavior in diverse engineering applications.

2 Background

The lattice Boltzmann method (LBM) has become a prominent computational tool for simulating fluid dynamics across various scales and complexities (Succi, 2018). It is based on the microscopic and kinetic theory of gases, allowing for the simulation of fluid dynamics by solving both the fluid dynamics and the constitutive equations of viscoelastic fluids (Fauzi, 2021; Ma et al., 2020). The LBM has been applied to a wide range of scenarios, from fully developed turbulence to multiphase micro-flows, and even quantum-relativistic subnuclear fluids (Succi, 2018). It has also been used to accurately compute airfoil flow and simulate plume dynamics (Wang et al., 2019; Mora & Yuen, 2017). Additionally, the LBM has been employed in the evaluation of the finite element lattice Boltzmann

method for binary fluid flows, demonstrating its versatility in handling complex fluid dynamics scenarios (Matin et al., 2017).

The importance of fluid dynamics simulation using the lattice Boltzmann method lies in its ability to provide efficient and accurate solutions for a wide variety of fluid flow problems, including those involving complex geometries (Zhu et al., 2020; Ma et al., 2020). The method has been utilized to study non-Newtonian flexible capsule flows in microchannels and to model the dynamics of self-propelled flexible swimming bodies, showcasing its applicability to diverse fluid dynamics phenomena (Ma et al., 2020; Luo et al., 2017). Furthermore, the LBM has been employed in the simulation of plume dynamics and the hydrodynamic repulsion of microparticles from micro-rough surfaces, demonstrating its relevance in both environmental and biological applications (Mora & Yuen, 2017; Belyaev, 2017).

Moreover, the lattice Boltzmann method has been used in conjunction with other mesoscopic approaches, such as multiparticle collision dynamics, to design flexible and efficient multiscale schemes for fluid dynamics simulations (Montessori et al., 2020). This highlights its potential for addressing the limitations of the LBM in providing accurate physical information due to a lack of resolution, particularly in scenarios involving thin films and interacting bubbles (Montessori et al., 2020).

In summary, the lattice Boltzmann method plays a crucial role in fluid dynamics simulation, offering a versatile and efficient computational tool for studying a wide range of fluid flow phenomena, from macroscopic to microscopic scales, and across various complexities and geometries.

3 Methodology

In the investigation of fluid dynamics, we employ the Lattice Boltzmann method to model the flow of fluid around a cylindrical structure. This methodology stands out as a sophisticated and streamlined approach to fluid simulation. In contrast to directly evolving the fluid equations, such as the Navier-Stokes equations, the Lattice Boltzmann method intricately simulates microscopic particles situated on a lattice. This simulation involves discrete streaming and collision processes, showcasing the method's efficacy in compressing the intricate physics of the microscopic domain onto the lattice, which inherently possesses restricted degrees of freedom. The method's ingenuity lies in its ability to handle the complex high-dimensionality of microscopic interactions through this lattice-based representation.

3.1 Lattice

Commencing our analysis, we delve into the microscopic depiction of a fluid residing on a lattice. In this particular investigation, our focus is directed toward a 2-dimensional lattice characterized by 9 feasible velocities at each lattice site,

conforming to the $D2Q9$ model. This lattice arrangement encompasses 4 cardinal connections—North, South, East, and West—along with 4 diagonal connections, and a singular connection from a node to itself, symbolizing zero velocity. Additionally, each lattice site is assigned a weight, denoted as w_i. The fundamental constitution of the fluid's microscopic entities finds expression through the distribution function, denoted as $f(x, v)$. This function serves to articulate the phase-space density of fluid particles situated at the spatial location x, traversing with the velocity v.

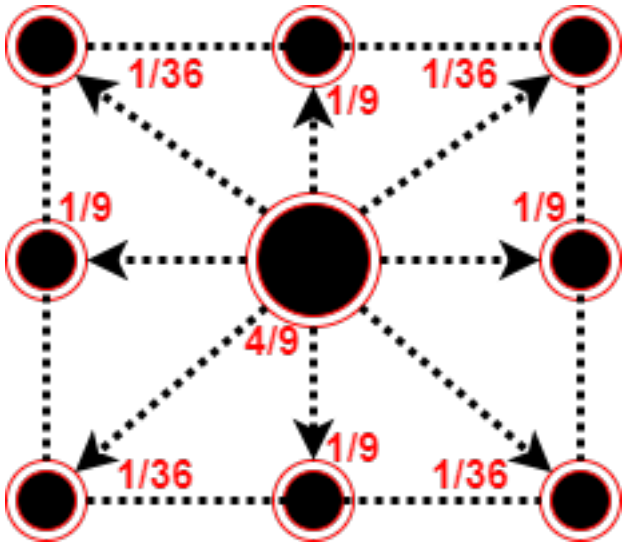

Fig. 1: Structure of D2Q9 Lattice with their corresponding weights.

D2Q9 Lattice: The lattice model $D2Q9$ finds prominent application in the domain of computational fluid dynamics (CFD) simulations, offering a structured framework for the representation of fluid behavior. This model delineates a two-dimensional grid featuring nine distinct velocity directions. Each direction is meticulously associated with a specific weight and velocity vector, contributing to the comprehensive characterization of fluid dynamics within a discrete lattice structure. D2Q9 stands as a widely employed paradigm for the simulation of fluid flow and various other physical phenomena manifesting in a two-dimensional spatial context.

3.2 Particle Movement

The dynamic behavior of particles within the fluidic system is characterized by two fundamental processes: streaming and collision. This intricate behavior is

effectively encapsulated through the BGK (Bhatnagar-Gross-Krook) approximation, a mathematical model strategically employed to simplify the Boltzmann equation, offering insights into the molecular-level interactions within a gas. Originating from the collaborative efforts of Philippe Burdeau, Carlo Cercignani, and Igor G. Kondratiev, the BGK approximation posits the representation of gas molecules through a singular distribution function. This function undergoes evolution under the influence of a streamlined collision operator, presenting a simplified yet accurate portrayal of gas dynamics. Widely embraced in computational fluid dynamics (CFD) simulations, the BGK approximation emerges as a computationally economical alternative to solving the complete Boltzmann equation, rendering it particularly advantageous for addressing intricate flow challenges in diverse engineering applications. This behavior can be captured by the BGK approximation:

$$\left(\partial_t + v \cdot \nabla\right) f = -\frac{f - f^{eq}}{\tau} \tag{1}$$

In the context of the BGK approximation, the modeling of fluid dynamics involves a distinct separation between streaming, depicted on the left-hand side, and the approximation of collision processes on the right-hand side. Herein, the parameter τ delineates the timescale governing the occurrence of collisions, influencing the evolution of the distribution function f. The distribution function tends towards a state of equilibrium denoted as f^{eq}, signifying the stabilized state resulting from the interplay of streaming and collision phenomena. The equation may be discretized onto the lattice as follows:

$$F_i\left(x_i + v_i \Delta t, t + \Delta t\right) - F_i\left(x_i, t\right) = \; - \frac{F_i\left(x_i, t\right) - F_i^{eq}\left(x_i, t\right)}{\tau} \tag{2}$$

where i denotes 1 out of the 9 lattice directions (with velocity v_i).

The extraction of fluid variables at individual lattice sites is facilitated by computing the moments of the discrete distribution function. A pertinent example is the determination of density, whereby the analysis involves deriving specific mathematical expressions from the distribution function to encapsulate the macroscopic properties of the fluid system.

$$\rho = \sum F_i \tag{3}$$

and **momentum**:

$$\rho u = \sum F_i v_i \tag{4}$$

The summation extends across all lattice directions.

Demonstrably, this formulation serves as an approximation to the Navier-Stokes fluid equations, offering a methodical representation that captures the essential dynamics of fluid behavior within the lattice structure (Wagner et. al., 2008).

3.3 Streaming

The initial phase of the Lattice Boltzmann method involves the streaming of particles, a process characterized by its remarkable simplicity. Conceptually, this entails the displacement of the value F_i at each lattice site in accordance with the specified direction i, effectively shifting it to the adjacent lattice site along the corresponding connection. In the conventional usage of the Lattice Boltzmann method, where $\Delta t = \Delta x = 1$, this streaming operation occurs seamlessly, with velocities (0,0), (0,1), (0,-1), (1,0), (-1,0), (1,1), (1,-1), (-1,1), (-1,-1) governing the displacement of values, thereby establishing a standardized convention for the method.

3.4 Collisions

Subsequently, the establishment of the equilibrium state following collisions is contingent upon the equation of state governing the fluid model. In the context of this illustration, we consider an isothermal fluid, characterized by a constant temperature and an unvarying sound speed. Adopting widely accepted conventions, we set the lattice speed as c=1, corresponding to a sound speed^2 of 1/3. The equilibrium state is succinctly expressed as follows:

$$F_i^{eq} = \omega_i \rho (1 + 3\,(v_i \cdot u) + \frac{9}{2}\,(v_i \cdot u)^2 + \frac{3}{2}\,(u \cdot u)) \tag{5}$$

which corresponds to the isothermal Navier-Stokes equations with a dynamic viscosity:

$$\mu = \rho \left(\tau - \frac{1}{2}\right) \Delta t \tag{6}$$

3.5 Boundary

The integration of boundary conditions within the Lattice Boltzmann framework is executed at the microscopic level. In the context of our simulation, where the presence of a solid cylinder is envisaged, specific lattice sites associated with this cylinder are designated for distinct treatment. In this instance, we opt for reflective boundary conditions, where the behavior of particles differs. Unlike the typical collision process leading to equilibrium, particles encountering the solid boundary undergo a distinctive response – a straightforward reflection. This is achieved by interchanging lattice directions, denoted by indices i and j, corresponding to opposite orientations.

$$F_i \leftrightarrow F_j \tag{7}$$

3.6 Lattice Boltzmann Method

Concluding the conceptual overview, the subsequent code amalgamates the defined lattice structure and initial conditions for F_i. The orchestrated sequence of

streaming and collision, coupled with boundary operations, orchestrates the evolution of the system. Notably, the constrained microscopic framework showcased in this code demonstrates a remarkable capability to emulate and encapsulate the complex macroscopic behavior exhibited by fluid systems.

4 Implementation

In the pursuit of simulating fluid dynamics using the Lattice Boltzmann method, a comprehensive implementation unfolds through distinct stages, each contributing to the refinement of the model. Herein, the simulation speed is a crucial parameter, denoted by the variable 'plot_every' with a value of 200, indicating the interval for visualizing results. All the coding parts have been done in Python3 using Numpy and Matplotlib for visualization.

The initial step establishes the lattice dimensions and temporal parameters, defining the lattice speeds, weights, and the initial conditions for the distribution function F_i. The lattice is initialized with a random perturbation, and a solid cylinder is introduced by flagging relevant lattice sites. This foundational setup lays the groundwork for subsequent stages.

The second step introduces the streaming and collision processes, reflecting the core dynamics of the Lattice Boltzmann method. Employing Neumann boundary conditions, the streaming operation shifts the distribution function values at each lattice site, while the collision phase updates the system by iterating over the lattice directions. Reflective boundary conditions are incorporated for lattice sites belonging to the solid cylinder, facilitating the reflection of particles.

The final implementation enriches the model by integrating a curl calculation to visualize the vorticity of the fluid flow. This enhancement involves computing the curl through finite differences in fluid velocities, providing insights into the rotational behavior of the simulated fluid. The visualization is achieved through the display of the resulting curl using a color map.

This sequential evolution from conceptualization to refined implementation underscores the prowess of the Lattice Boltzmann method in capturing macroscopic fluid behavior. The structured approach taken in these steps lays the foundation for comprehensive simulations and further exploration in the realm of computational fluid dynamics.

5 Result and Analysis

In the pursuit of simulating fluid dynamics through the Lattice Boltzmann Method (LBM) for computational fluid dynamics (CFD), a comprehensive implementation was undertaken. The simulation was configured to unfold over a spatial grid, comprising 400 cells in the x-direction and 100 cells in the y-direction. The chosen kinematic viscosity or timescale parameter, denoted as τ, was set at 0.53. The temporal evolution of the system spanned 10,000 iterations, providing a detailed exploration of fluid behavior.

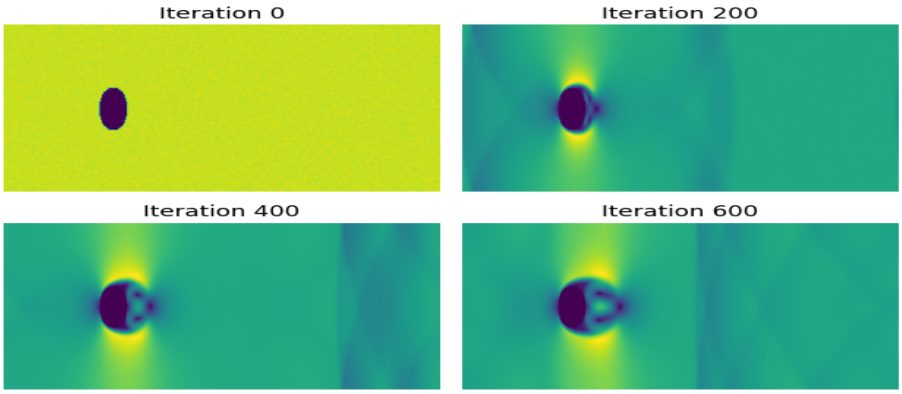

Fig. 2: Applied Lattice Boltzmann method. This corresponds to the magnitude of velocity where the yellow means a very high velocity and the dark purple means a very very low velocity right behind the cylinder.

The discretization of velocities in the lattice involved nine distinct speeds (cxs, cys), each associated with specific weights. The lattice velocities (cxs, cys) were organized in arrays, defining the discrete movements in the x and y directions. The corresponding weights delineated the likelihood of particle movement in a particular direction.

To initialize the system, random perturbations were introduced to ensure realistic fluid conditions. Notably, a mesoscopic velocity field (F) was generated with slight inconsistencies to emulate the inherent turbulence in fluid dynamics. Additionally, a directional bias was introduced by assigning a rightward velocity (2.3) to specific nodes, contributing to an overall flow in the simulation.

The simulation incorporated a cylindrical obstacle, strategically positioned within the grid. The obstacle was defined using a distance function, marking grid points within a specified radius as part of the cylinder. This modular approach allows for the adaptation of boundary conditions to various geometries.

The simulation unfolded through a series of steps, including streaming, collision, and the imposition of boundary conditions. Neumann boundary conditions were applied at the lattice edges, with absorbing boundary conditions implemented to minimize artificial reflections and enhance simulation stability.

A crucial aspect of the simulation involved handling collisions with the cylinder. Upon collision, velocities inside the cylinder were adjusted to their opposite values, ensuring an accurate representation of fluid dynamics around obstacles.

Fluid variables such as density (ρ) and momentum (ux, uy) were calculated to characterize the system's macroscopic behavior. Absorbing boundary conditions were employed to mitigate undesired reflections, particularly at the right boundary.

The simulation's main loop iterated through time steps, integrating streaming, collision, and boundary adjustments. Fluid equilibrium (Feq) was computed

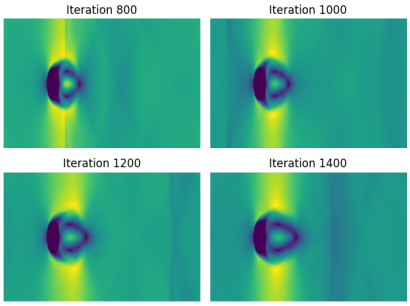

(a) Simulated scenario after 1400th iteration on normal Lattice Boltzmann method.

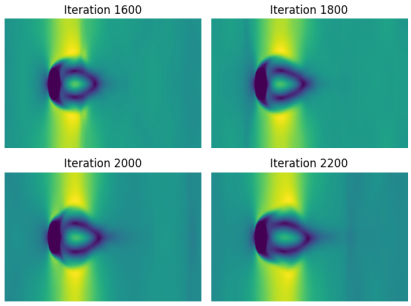

(b) Simulated scenario after 2200th iteration on normal Lattice Boltzmann method.

Fig. 3: The vortex has been visible clearly and swirling starts. The present limitation of this approach is the boundary problem of the collision. The observation clarifies that there is some rippling and this ripple happened due to a reflective boundary. Because of its reflective nature, the fluid mirrors the opposite wall of the boundary. We can observe a strong yellow zone over the top and the bottom of the cylinder which is responsible for moving the energy stream downward.

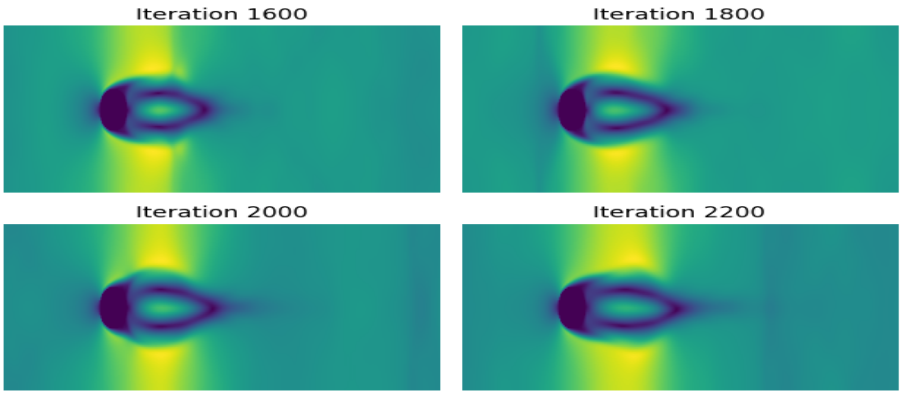

Fig. 4: Simulated scenario after 2200th iteration on normal Lattice Boltzmann method. The vortex has been visible clearly and swivelling starts. The present limitation of this approach is the boundary problem of the collision. The observation clarifies that there is some rippling and this ripple happened due to a reflective boundary. Because of its reflective nature, the fluid mirrors the opposite wall of the boundary.

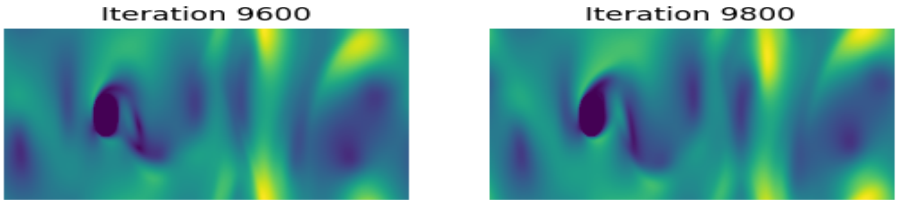

Fig. 5: Simulated scenario after 9800th iteration on normal Lattice Boltzmann method. We can observe that the fluid dynamics have completely mixed under the fixed boundary. The swirling gets mixed due to a reflective boundary problem as we can observe.

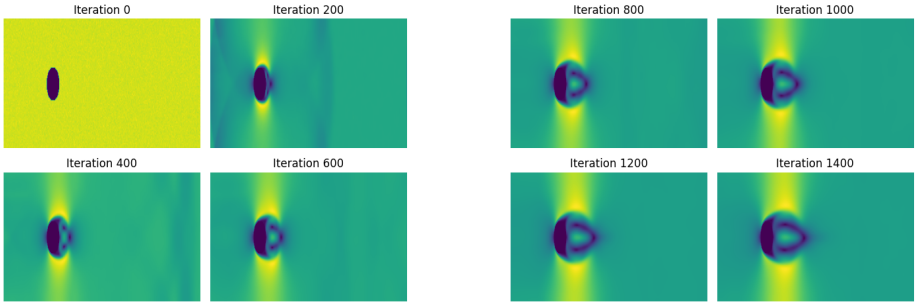

(a) (b)

Fig. 6: Simulated scenario after applying Lattice Boltzmann method with Neumann boundary condition. We can observe the Kármán Vortex clearly because the right values have been absorbed by the walls and we will get a much smoother simulation of all of the waves.

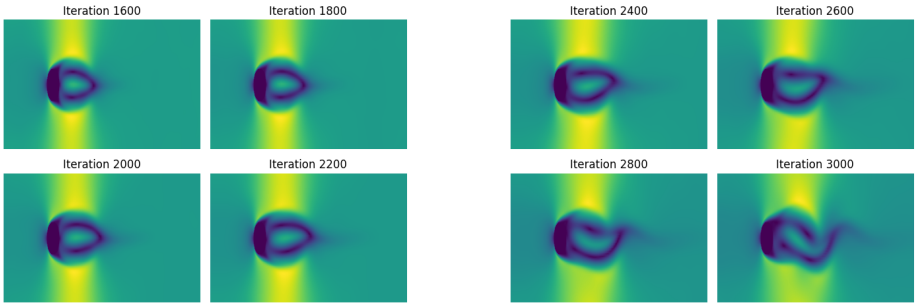

(a) The boundary condition on the top and the bottom wall has been implemented thus the reflection gets smoother.

(b) After 3000th iteration the first swirling found. The yellow shade shows the dynamics of fluid around the cylinder.

Fig. 7: When the fluid is getting hit by those waves from the top and bottom because it lets it reach these swirls much faster.

based on macroscopic variables, facilitating the update of lattice values according to the LBM equation.

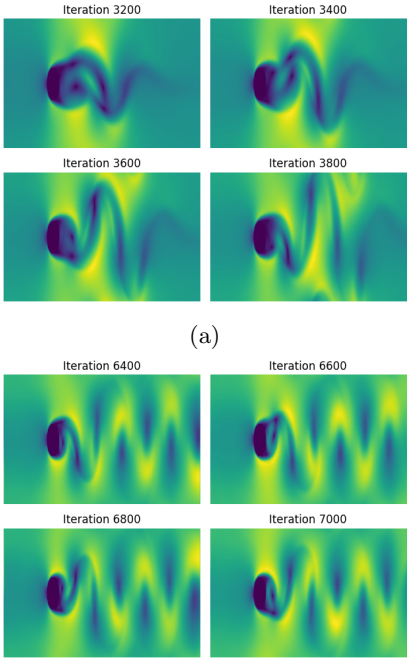

(c) Boundary condition applied. Observation till 7000th iteration.

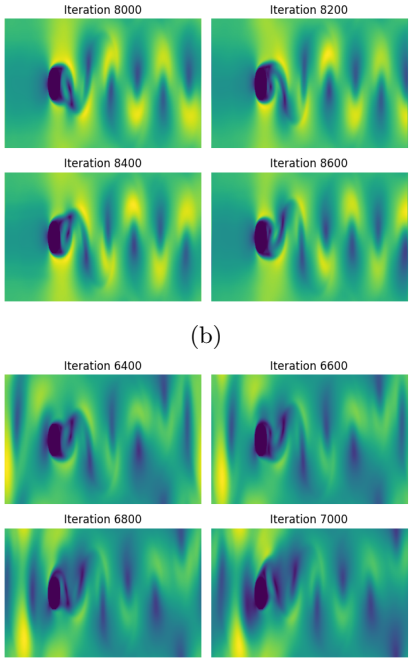

(d) Boundary condition not applied. Observation till 7000th iteration.

Fig. 8: We started to get some asymmetries because it seems to be that there is a bit more velocity in the top than there is in the bottom and we're starting to notice a little bit of concavity and it's going to start to swirl soon. In images (c) and (d) we can observe the difference in applying boundary conditions on every side of the environment. The side-by-side comparison shows the smoothness and the proper distribution of waves that generate the energy concavity at the top of the cylinder.

The results were visualized by plotting the magnitude of velocity and vorticity (curl). Absorbing boundary conditions effectively dampened unwanted reflections, allowing the emergence of Von Karman vortex shedding behind the cylinder. The vorticity plot provided insights into regions of high and low swirliness, highlighting the dynamic behavior of the fluid.

This modular and adaptable simulation framework lays the foundation for in-depth investigations into various fluid dynamics scenarios, offering a versatile tool for research and analysis. The nuanced interplay of LBM components provides a robust platform for exploring complex fluid phenomena.

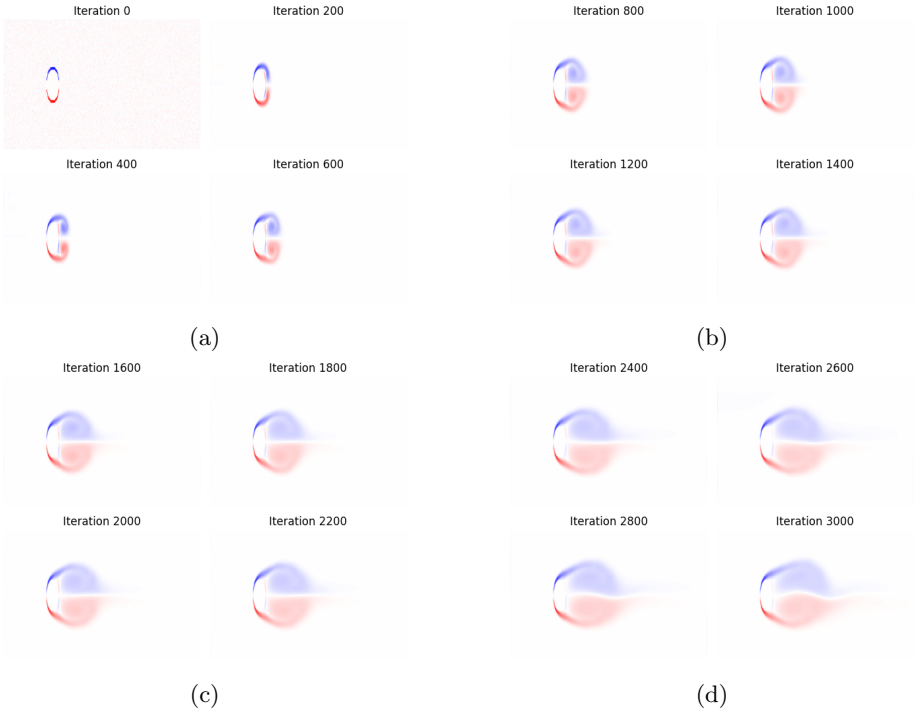

Fig. 9: We plot our curl and taking the curl of a vector field is simply a mathematical operation that just involves testing for points of essentially high swirliness and we calculated the points of high swirliness. The color map BWR gives red to positive values and blue to negative values. We can see that the plotting regions of high and low vorticity which create the swirl proper to understand the fluid dynamics and its flow.

The initial setup delineates a static cylindrical obstacle within a periodic domain, subjected to a unidirectional fluid flow. As the simulation progresses, the evolution of turbulence in the wake of the cylinder manifests the well-documented Kármán vortex street phenomenon.

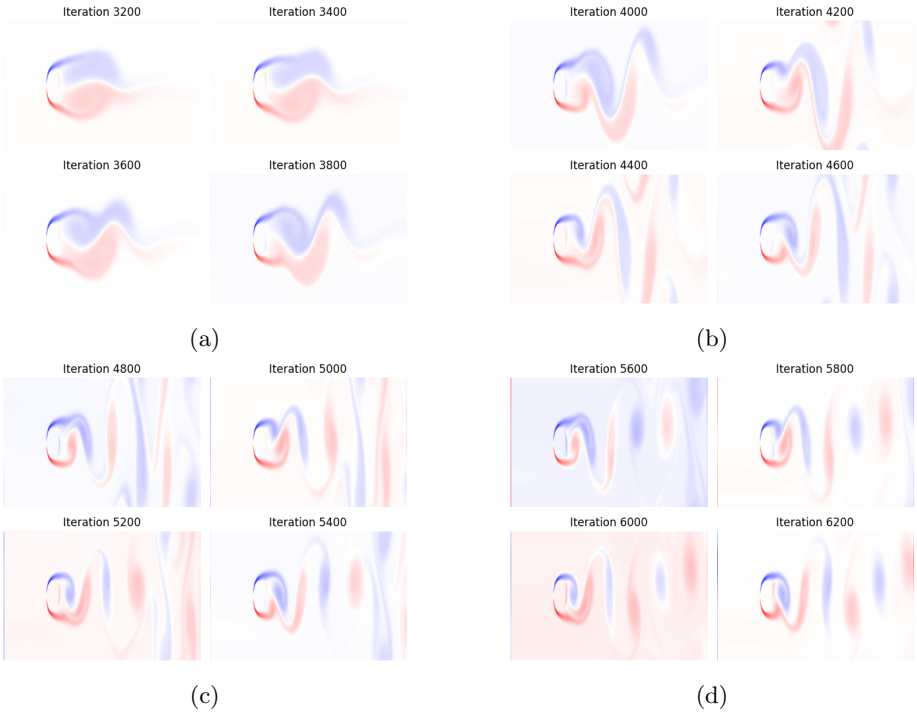

Fig. 10: The energy density shows the reason that golf balls have dents in them and aren't perfectly cylindrical or aren't perfectly spherical is that if they were perfectly spherical they would have this region of low velocity behind them. That region of low velocity causes a region of low pressure which sucks the golf ball back reducing its speed by having those little dimples golf balls can develop some turbulence along their walls and can help prevent it. We can see that we're starting to get the von Karman vortex stream as the imperfections from the randomness we input into our initial conditions have been mitigated.

Kármán Vortex Street Dynamics: The term "Kármán vortex street" characterizes a captivating phenomenon observed when a fluid, such as air or water, interacts with a solid object, resulting in a distinctive pattern of alternating vortices or swirling motions in the object's downstream wake. This phenomenon, named after the pioneering aerospace engineer Theodore von Kármán, has been a subject of study since its first description in the early 20th century.

The manifestation of a "vortex street" denotes the sequential shedding of vortices from the object as the fluid traverses its vicinity. This shedding arises from the intricate interplay between the fluid and the object, prompting the separation of the fluid and the formation of swirling motions.

The shed vortices follow an alternating pattern, with each vortex being released on opposing sides of the object. The consequential sequence of vortices creates a discernible street-like pattern in the downstream region, giving rise to the term "vortex street."

The Kármán vortex street phenomenon is ubiquitously observed in diverse natural and man-made scenarios, encompassing the airflow around structures like buildings, bridges, and vehicles, as well as water flow around marine vessels. Its occurrence can significantly impact flow dynamics, inducing effects such as heightened drag on the object, vibration, and audible noise.

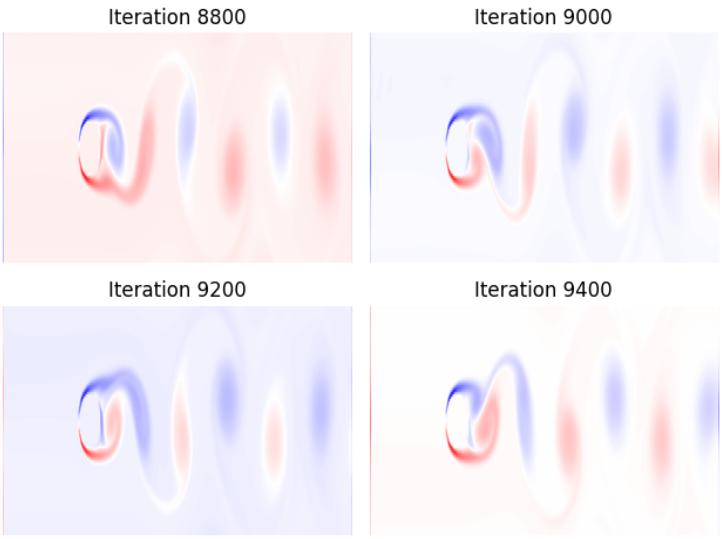

(a)

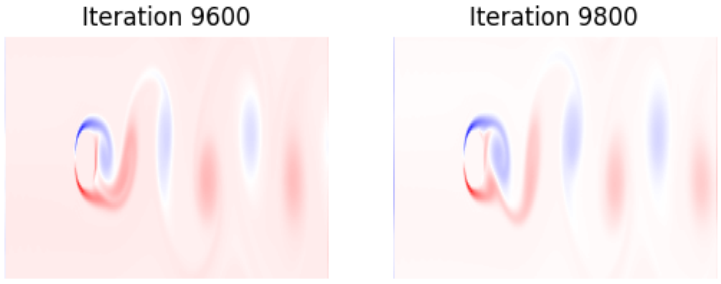

(b) After implementing the curl.

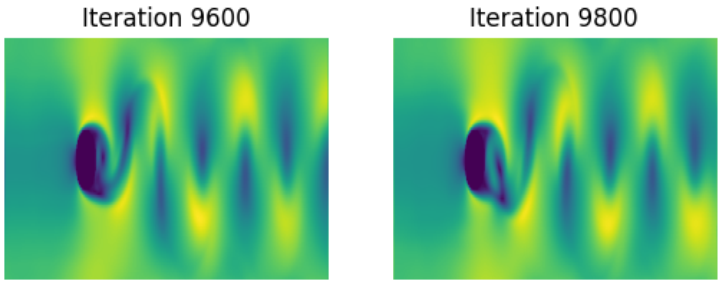

(c) Without implementing the curl.

Fig. 11: We can see the different energy streams in fig (a) which illustrates the environment of the cylindrical body sometimes gets positive and the other times negative. In Fig (b) and Fig (c) we can see the side-by-side comparison of the advantage of plotting curl where Fig (b) implements curl and gives a better understanding of fluid dynamics and Fig (c) shows the vortex only which is difficult to visualize the thin lines and requires much more technical understanding of the concept.

The comprehension and predictive modeling of Kármán vortex streets hold paramount importance in various engineering and scientific domains. Such understanding facilitates the optimization of structural designs and the enhancement of fluid flow efficiency. The real-time visualization of vorticity ($\omega=\nabla\times\mathrm{v}$) during the simulation provides a dynamic depiction of the Kármán vortex street, further contributing to the comprehensive exploration of fluid phenomena. The resultant figure serves as a visual representation of the intricate dynamics underlying this phenomenon in the context of the simulated flow past the cylindrical obstacle.

6 Conclusion

The Lattice Boltzmann method presents a versatile and widely applicable approach for simulating complex multi-fluid flows featuring intricate boundaries. However, it has inherent limitations, particularly in accurately representing highly compressible or supersonic flows. This drawback restricts its frequent application in computational astrophysics, where such flow conditions are prevalent. Nevertheless, the method finds extensive use in various other domains.

In the context of a numerical experiment involving the flow past a cylinder using the Lattice Boltzmann method, the impact of viscosity variation was investigated. Notably, the wake behind the cylinder exhibited turbulence as viscosity decreased, corresponding to higher Reynolds numbers.

Expanding the scope, a more intricate scenario was explored, studying wind flow around buildings within an urban setting. The Lattice Boltzmann method facilitated the seamless incorporation of buildings and modification of boundary conditions by flagging lattice sites, offering a straightforward approach. The simulation successfully identified regions where buildings influenced high wind velocities.

In conclusion, this analysis underscores the simplicity and efficacy of the Lattice Boltzmann approach in fluid dynamics, providing insight into the microscopic foundations of fluid behavior. Moving forward, future research could focus on refining the method's applicability to highly compressible flows, thereby enhancing its utility in astrophysical simulations. Additionally, exploring advancements for more intricate simulations involving complex geometries and boundary conditions holds promising avenues for further research in computational fluid dynamics.

References

1. Amirante, R., Moscatelli, P., & Catalano, L. (2007). Evaluation of the flow forces on a direct (single stage) proportional valve by means of a computational fluid dynamic analysis. Energy Conversion and Management, 48(3), 942-953. https://doi.org/10.1016/j.enconman.2006.08.024

2. Applebaum, M., Eppard, M., Hall, L., & Blevins, J. (2012). Protuberance aerodynamic loads for space launch vehicle systems using computational fluid dynamics. Journal of Spacecraft and Rockets, 49(5), 779-787. https://doi.org/10.2514/1.a32171
3. Aydin, K., Güler, O., & Keçebaş, A. (2017). Parameters affecting the performance of a plate heat exchanger using the cfd. Energy Research Journal, 8(2), 22-31. https://doi.org/10.3844/erjsp.2017.22.31
4. Chen, Q. (2009). Real-time or faster-than-real-time simulation of airflow in buildings. Indoor Air, 19(1), 33-44. https://doi.org/10.1111/j.1600-0668.2008.00559.x
5. Chinnarasri, C., Kositgittiwong, D., & Julien, P. (2014). Model of flow over spillways by computational fluid dynamics. Proceedings of the Institution of Civil Engineers - Water Management, 167(3), 164-175. https://doi.org/10.1680/wama.12.00034
6. Fang, J., Zhu, J., Fu, C., & He, Y. (2023). Prediction of centrifugal compressor performance curves based on multi-task gaussian process.. https://doi.org/10.1117/12.2681868
7. Hu, C. and Zhang, X. (2018). A computational framework for predicting the combustion of energetic materials in an expanding chamber. International Journal of Numerical Methods for Heat & Fluid Flow, 28(11), 2606-2619. https://doi.org/10.1108/hff-02-2018-0052
8. Kim, B., Azevedo, V., Thuerey, N., Kim, T., Groß, M., & Solenthaler, B. (2019). Deep fluids: a generative network for parameterized fluid simulations. Computer Graphics Forum, 38(2), 59-70. https://doi.org/10.1111/cgf.13619
9. Lin, S., Stanton, S., Lian, W., & Tie-jun, W. (2011). Battery modeling based on the coupling of electrical circuit and computational fluid dynamics.. https://doi.org/10.1109/ecce.2011.6064119
10. Liu, W., Jin, M., Chen, C., & Chen, Q. (2015). Optimization of air supply location, size, and parameters in enclosed environments using a computational fluid dynamics-based adjoint method. Journal of Building Performance Simulation, 9(2), 149-161. https://doi.org/10.1080/19401493.2015.1006525
11. Lu, Y., Agrawal, M., & Skeels, H. (2011). Cfd thermal analysis of subsea equipment and experimental validation.. https://doi.org/10.4043/21553-ms
12. Macgregor, S., Newnes, L., Li, M., Staniforth, J., Tobyn, M., Kay, G., ... & Page, T. (1999). The application of computational fluid dynamics to the development of a pharmaceutical processor. Proceedings of the Institution of Mechanical Engineers Part B Journal of Engineering Manufacture, 213(7), 737-740. https://doi.org/10.1243/0954405991517155
13. Ochi, A., Ibrahim, M., & Nakamura, Y. (2010). Computational fluid dynamics validation study of wake-capturing capability for flat-plate wake. Journal of Aircraft, 47(2), 441-449. https://doi.org/10.2514/1.33502
14. Orfánus, M. and Rumann, J. (2019). Air entrainment and free surface modeling of fully turbulent flow near the broad-crested weirs. Pollack Periodica, 14(3), 153-164. https://doi.org/10.1556/606.2019.14.3.15
15. Pratama, H. and Bramantya, M. (2018). Numerical studies influence configuration fairing flap track airfoil type naca 4412 and naca 6412 character unmanned aerial vehicle (uav). Matec Web of Conferences, 197, 08017. https://doi.org/10.1051/matecconf/201819708017
16. Sforza, D., Putman, C., & Cebral, J. (2011). Computational fluid dynamics in brain aneurysms. International Journal for Numerical Methods in Biomedical Engineering, 28(6-7), 801-808. https://doi.org/10.1002/cnm.1481

17. Taxy, S. and Lebreton, E. (2004). Use of computational fluid dynamics to investigate the impact of cold spots on subsea insulation performance.. https://doi.org/10.4043/16502-ms
18. Wang, X. (2012). Computational fluid dynamics predictions of stability derivatives for airship. Journal of Aircraft, 49(3), 933-940. https://doi.org/10.2514/1.c031634
19. Xu, Y., Guan, Z., Liu, Y., Liu, X., Zhang, H., & Xu, C. (2014). Structural optimization of downhole float valve via computational fluid dynamics. Engineering Failure Analysis, 44, 85-94. https://doi.org/10.1016/j.engfailanal.2014.04.033
20. Yu, H., Lin, J., & Liu, T. (2017). Application of computational fluid dynamics (cfd) in contaminant monitoring and analysis. Destech Transactions on Environment Energy and Earth Science, (icesee). https://doi.org/10.12783/dteees/icesee2017/7863
21. Zhu, M., Zhao, S., Li, J., & Dong, P. (2018). Computational fluid dynamics and experimental analysis on flow rate and torques of a servo direct drive rotary control valve. Proceedings of the Institution of Mechanical Engineers Part C Journal of Mechanical Engineering Science, 233(1), 213-226. https://doi.org/10.1177/0954406218756449
22. Belyaev, A. (2017). Hydrodynamic repulsion of spheroidal microparticles from micro-rough surfaces. Plos One, 12(8), e0183093. https://doi.org/10.1371/journal.pone.0183093
23. Fauzi, U. (2021). Lid-driven cavity for mantle convection modelling using lattice boltzmann method. Indonesian Journal of Physics, 32(1), 21-28. https://doi.org/10.5614/ijp.v32i1.307
24. Luo, Y., Wu, T., & Qi, D. (2017). Lattice-boltzmann lattice-spring simulations of flexibility and inertial effects on deformation and cruising reversal of self-propelled flexible swimming bodies. Computers & Fluids, 155, 89-102. https://doi.org/10.1016/j.compfluid.2017.05.016
25. Ma, J., Wang, L., & Tian, F. (2020). Ib-lbm study of non-newtonian flexible capsule flows in contraction-expansion microchannels.. https://doi.org/10.14264/6e15e3d
26. Ma, J., Wang, Z., Young, J., Lai, J., Sui, Y., & Tian, F. (2020). An immersed boundary-lattice boltzmann method for fluid-structure interaction problems involving viscoelastic fluids and complex geometries. Journal of Computational Physics, 415, 109487. https://doi.org/10.1016/j.jcp.2020.109487
27. Matin, R., Misztal, M., Hernandez-Garcia, A., & Mathiesen, J. (2017). Evaluation of the finite element lattice boltzmann method for binary fluid flows. Computers & Mathematics With Applications, 74(2), 281-291. https://doi.org/10.1016/j.camwa.2017.04.027
28. Montessori, A., Tiribocchi, A., Lauricella, M., & Succi, S. (2020). A coupled lattice boltzmann-multiparticle collision method for multi-resolution hydrodynamics.. https://doi.org/10.48550/arxiv.2004.00304
29. Mora, P. and Yuen, D. (2017). Simulation of plume dynamics by the lattice boltzmann method. Geophysical Journal International, 210(3), 1932-1937. https://doi.org/10.1093/gji/ggx279
30. Succi, S. (2018). The lattice boltzmann equation.. https://doi.org/10.1093/oso/9780199592357.001.0001
31. Wang, L., Zhang, X., Zhu, W., Xu, K., Wu, W., Chu, X., ... & Zhang, W. (2019). Accurate computation of airfoil flow based on the lattice boltzmann method. Applied Sciences, 9(10), 2000. https://doi.org/10.3390/app9102000
32. Zhu, H., Xu, X., Huang, G., Qin, Z., & Wen, B. (2020). An efficient graphics processing unit scheme for complex geometry simulations using the lattice boltzmann method. Ieee Access, 8, 185158-185168. https://doi.org/10.1109/access.2020.3029800

33. Wagner, A. J. (2008). A practical introduction to the lattice Boltzmann method. Adt. notes for Statistical Mechanics, 463, 663.